

Mapping the I κ B Kinase β (IKK β)-binding Interface of the B14 Protein, a Vaccinia Virus Inhibitor of IKK β -mediated Activation of Nuclear Factor κ B^{*[5]}

Received for publication, February 15, 2011, and in revised form, April 6, 2011. Published, JBC Papers in Press, April 7, 2011, DOI 10.1074/jbc.M111.231381

Camilla T. O. Benfield[‡], Daniel S. Mansur^{†1}, Laura E. McCoy^{‡2}, Brian J. Ferguson[‡], Mohammad W. Bahar[§], Asa P. Oldring^{§3}, Jonathan M. Grimes^{§¶}, David I. Stuart^{§¶4}, Stephen C. Graham^{§||5}, and Geoffrey L. Smith^{‡6}

From the [‡]Section of Virology, Department of Medicine, Imperial College London, St Mary's Campus, Norfolk Place, London W2 1PG, the [§]Division of Structural Biology and Oxford Protein Production Facility, Wellcome Trust Centre for Human Genetics, University of Oxford, Oxford OX3 7BN, the [¶]Science Division, Diamond Light Source Ltd., Diamond House, Harwell Science and Innovation Campus, Didcot OX11 0DE, and the ^{||}Cambridge Institute for Medical Research and Department of Clinical Biochemistry, University of Cambridge and Addenbrooke's Hospital, Hills Road, Cambridge CB2 0XY, United Kingdom

The I κ B kinase (IKK) complex regulates activation of NF- κ B, a critical transcription factor in mediating inflammatory and immune responses. Not surprisingly, therefore, many viruses seek to inhibit NF- κ B activation. The vaccinia virus B14 protein contributes to virus virulence by binding to the IKK β subunit of the IKK complex and preventing NF- κ B activation in response to pro-inflammatory stimuli. Previous crystallographic studies showed that the B14 protein has a Bcl-2-like fold and forms homodimers in the crystal. However, multi-angle light scattering indicated that B14 is in monomer-dimer equilibrium in solution. This transient self-association suggested that the hydrophobic dimerization interface of B14 might also mediate its interaction with IKK β , and this was investigated by introducing amino acid substitutions on the dimer interface. One mutant (Y35E) was entirely monomeric but still co-immunoprecipitated with IKK β and blocked both NF- κ B nuclear translocation and NF- κ B-dependent gene expression. Therefore, B14 homodimerization is nonessential for binding and inhibition of IKK β . In contrast, a second monomeric mutant (F130K) neither bound IKK β nor inhibited NF- κ B-dependent gene expression, demonstrating that this residue is required for the B14-IKK β interaction. Thus, the dimerization and IKK β -binding interfaces overlap and lie on a surface used for protein-protein interactions in many viral and cellular Bcl-2-like proteins.

NF- κ B is a critical transcription factor that regulates many important cellular processes, such as differentiation, apoptosis, and the inflammatory response to infection. NF- κ B is composed of homo- or heterodimers of Rel domain family proteins (e.g. p65, RelB, and p50) and is maintained in an inactive state within the cytosol via interaction with I κ B α , the inhibitor of NF- κ B (1). Phosphorylation of two serine residues on I κ B α marks it for ubiquitin-mediated proteasomal degradation, and consequently, the released NF- κ B dimer translocates to the nucleus, where it binds its cognate κ B consensus sequences (2–4). The kinase that phosphorylates I κ B α is the I κ B kinase (IKK)⁷ complex (5), a heterotrimer composed of the IKK α and IKK β subunits and the regulatory subunit IKK γ (also known as NEMO) (6, 7). Several signaling pathways that lead to NF- κ B activation converge at the IKK complex, which is therefore a key regulator of NF- κ B activation. NF- κ B activation is initiated by pro-inflammatory cytokines (such as TNF α and IL-1 β), by Toll-like receptor ligands, or by the recognition of pathogen-associated molecular patterns produced during infection, and most of these pathways require IKK β (8). To become activated, IKK β is phosphorylated by upstream kinases, such as TAK1 (TGF β -activated kinase-1), on Ser-177 and Ser-181 located in an activation loop (5, 9). This phosphorylation stimulates the kinase activity of IKK β via a conformational rearrangement (10).

NF- κ B-dependent gene expression is very important for activation of the inflammatory and immune responses to virus infection. Accordingly, it is not surprising that viruses have evolved countermeasures to block NF- κ B activation. Large DNA viruses in particular, such as herpesviruses and poxviruses, have multiple strategies for blocking NF- κ B activation (for review, see Ref. 11).

Vaccinia virus (VACV) is an orthopoxvirus and the vaccine used to eradicate smallpox. It replicates in the cytoplasm and encodes numerous proteins that block the host response to infection, including inhibitors of NF- κ B. VACV strategies to antagonize NF- κ B activation include expression of (i) proteins that are secreted from the infected cells and that bind and

* This work was supported in part by Wellcome Trust Grant 075491/Z/04, the Conselho Nacional de Desenvolvimento Científico e Tecnológico (CNPq, Brazil; to D. S. M.), the Poxvirus T Cell Vaccine Discovery Consortium (PTVDC) under the Collaboration for AIDS Vaccine Discovery with support from the Bill and Melinda Gates Foundation (to L. E. M.), the Medical Research Council (United Kingdom), and European Commission Contract 031220FP6 (SPINE2-COMPLEXES).

[5] The on-line version of this article (available at <http://www.jbc.org>) contains supplemental Equations 1–15, Table S1, Figs. S1 and S2, and a reference.

Author's Choice—Final version full access.

¹ Present address: Dept. de Microbiologia, Imunologia e Parasitologia-MIP/CCB/UFSC, Campus Universitário da Trindade, Florianópolis, Caixa Postal 476, CEP 88.040-970, SC, Brazil.

² Present address: Wohl Virion Centre and MRC Centre for Medical Molecular Virology, Div. of Infection and Immunity, University College London, London W1T 4JF, UK.

³ Present address: Thermo Fisher Scientific, Basingstoke RG24 8PW, UK.

⁴ Supported by the Medical Research Council (United Kingdom).

⁵ 1851 Research Fellow. To whom correspondence may be addressed. E-mail: scg34@cam.ac.uk.

⁶ Wellcome Trust Principal Research Fellow. To whom correspondence may be addressed. E-mail: geoffrey.l.smith@imperial.ac.uk.

⁷ The abbreviations used are: IKK, I κ B kinase; VACV, vaccinia virus; MALS, multi-angle light scattering; SEC, size-exclusion chromatography.

Monomeric VACV B14 Binds IKK β on Its Dimerization Interface

sequester agonists of the NF- κ B pathway, such as IL-1 β and TNF α (12, 13), and (ii) intracellular inhibitors of signaling molecules, such as VACV proteins A52 (14, 15), A46 (14, 16), K1 (17), K7 (18), N1 (19), M2 (20), and B14 (21).

The VACV strain Western Reserve gene *B14R* is expressed early during infection and encodes a 15-kDa acidic protein that is present in the cytosol (22, 23). The B14 protein is nonessential for virus replication in cell culture, but a deletion mutant lacking the *B14R* gene was attenuated in a mouse intradermal model compared with control viruses, and the attenuated phenotype was characterized by an increased local inflammatory response to infection (22). The B14 protein functions by binding to the IKK complex via an interaction with IKK β and preventing the phosphorylation of IKK β on its activation loop (21). Consequently, IKK β is not activated and fails to phosphorylate I κ B α , leaving I κ B α able to retain NF- κ B in the cytoplasm. Thus, B14 inhibits NF- κ B-dependent signaling in response to several inflammatory stimuli (e.g. TNF α , IL-1, poly(I:C), and phorbol myristate acetate) (21). Further evidence that B14 inhibits IKK β by inhibiting its phosphorylation (rather than its kinase activity) was obtained by showing that B14 cannot inhibit constitutively activated IKK β (S177E/S181E) (21). It has also been shown that B14 does not interfere with the assembly of the IKK complex (21).

The structure of B14 was solved by x-ray crystallography and revealed that B14 comprises seven α -helices and adopts a Bcl-2-like fold (24). The crystal structures of four other VACV proteins with a Bcl-2 structure have also been solved: N1 (25, 26), A52 (24), F1 (27), and K7 (28) (for review, see Ref. 29). Of these, only F1 and N1 have anti-apoptotic activity, and consistent with this, the others (B14, A52, and K7) lack a binding groove for pro-apoptotic BH3 peptides (24, 28). Instead, these proteins have evolved to regulate pro-inflammatory intracellular signaling cascades by binding cellular proteins that function in those pathways. Interestingly, N1 can also inhibit pro-inflammatory signaling cascades and thus appears to have a dual function (24, 26). A common feature of VACV Bcl-2-like proteins is their propensity to form homodimers. Whereas F1 forms an intimate "helix-swapped" dimer, where helix 1 derives from the other molecule in the dimer (27), B14, A52, and N1 all homodimerize using a conserved face formed by helices 1 and 6 plus residues N-terminal to helix 1 (we have termed this binding surface the "1–6 face") (24–26, 30).

Here, we sought to identify the region of B14 that binds IKK β and assessed the importance of dimer formation by the introduction of specific mutations on the B14 dimer interface. These mutants were assessed for their ability to form dimers, bind IKK β , and inhibit NF- κ B-dependent gene expression. We show that the ability to bind IKK β and block NF- κ B activation is not dependent upon B14 dimerization but rather that the dimerization and IKK β -binding interfaces overlap and that utilization of this surface for protein-protein interactions is a common feature of many viral and cellular Bcl-2-like proteins.

EXPERIMENTAL PROCEDURES

Protein Production and Characterization—Point mutations were introduced into the pET28a vector carrying B14 (24) by QuikChangeTM site-directed mutagenesis (Stratagene) using

the manufacturer's instructions and primers listed in [supplemental Table SI](#). The fidelity of all alleles was confirmed by DNA sequencing. N-terminally His₆-tagged wild-type and mutant B14 were overexpressed and purified by nickel affinity and size-exclusion chromatography as described (24). To confirm normal folding, the molar ellipticity of wild-type and mutant B14 (0.6 mg/ml) in 50 mM phosphate (pH 7.5) was recorded between 190 and 260 nm using a Jasco J-810 spectropolarimeter. The mass of wild-type B14 was confirmed by mass spectroscopy (data not shown).

Multi-angle light scattering (MALS) experiments were performed immediately following size-exclusion chromatography by inline measurement of static light scattering (DAWN HELEOS II, Wyatt Technology), differential refractive index (Optilab rEX, Wyatt Technology), and ultraviolet absorbance (Agilent 1200 UV, Agilent Technologies). Samples (100 μ l) were injected onto an analytical Superdex 75 10/300 gel filtration column (GE Healthcare) equilibrated in 50 mM Tris (pH 8.5), 150 mM NaCl, and 2 mM 2-mercaptoethanol at a flow rate of 0.5 ml/min. The dissociation constant (K_D) of wild-type B14 was determined by measuring the weight average molar mass across a range of protein concentrations (injected at 0.3–4.7 mg/ml) and fitting the data by nonlinear regression to Equation 1,

$$M_w = M_r \left(\frac{8[M]_T + K_D - \sqrt{K_D^2 + 8[M]_T K_D}}{4[M]_T} \right) \quad (\text{Eq. 1})$$

where M_w is the weight average molar mass (31), $[M]_T$ is the molar concentration of protein (as measured by change in refractive index), and M_r is molecular mass (19,545 kDa for N-terminally His-tagged B14). For derivation of this equation, see the [supplemental data](#). MALS data were analyzed using ASTRA V (Wyatt Technology), nonlinear regression analysis was performed using Prism 5 (GraphPad Software), structures were superposed with SSM (32), protein interaction interfaces were analyzed using PDBEPIA (33), and molecular graphics were generated using PyMOL (DeLano Scientific).

Cells, Plasmids, and Antibodies—HEK293T (human embryonic kidney) cells were maintained in DMEM (Invitrogen) supplemented with 10% FBS, penicillin, and streptomycin. HeLa cells were grown in minimal essential medium (Invitrogen) supplemented with nonessential amino acids (Sigma), 10% FBS, penicillin, and streptomycin. All cells were grown at 37 °C in an atmosphere of 5% carbon dioxide.

The NF- κ B-luciferase reporter plasmid and the thymidine kinase-driven *Renilla* luciferase plasmid (pRL-TK) were described previously (21). Mutations were introduced into the pCI vector carrying FLAG-tagged B14 (21) by QuikChangeTM site-directed mutagenesis as described above. A plasmid expressing N-terminally HA-tagged IKK β was kindly provided by Dr. Alain Chariot (University of Liège).

For immunoblotting, mouse monoclonal anti-FLAG (F3165, Sigma), mouse monoclonal anti-tubulin (DM1A, Millipore), and rabbit polyclonal anti-HA (H6908, Sigma) antibodies were used. For immunoprecipitation, monoclonal anti-HA antibody (monoHA.11, Covance) or the isotype-matched anti-CD45 antibody (sc-1178, Santa Cruz Biotechnology) was used. For

Monomeric VACV B14 Binds IKK β on Its Dimerization Interface

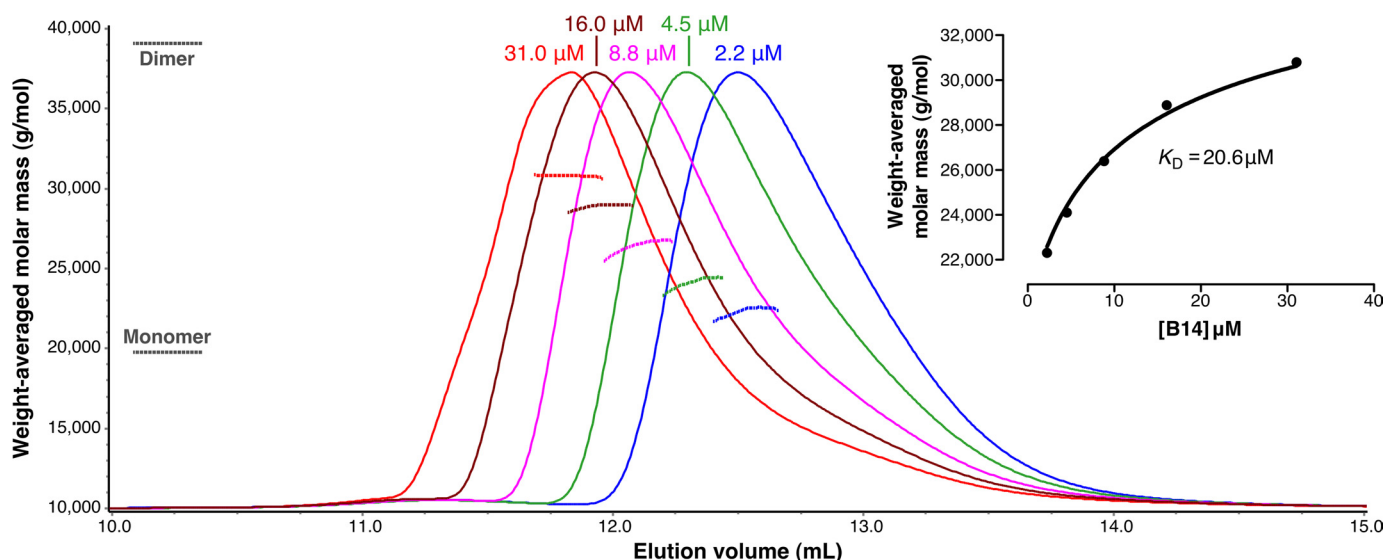


FIGURE 1. **B14 is in monomer-dimer equilibrium.** The weight average molar mass (dotted lines) is shown across the elution profile ($A_{280\text{ nm}}$ scaled so all peaks are the same height; solid lines) of pure B14 subjected to SEC-MALS at five different concentrations. The inset shows the weight average molar mass plotted as a function of concentration, with the solid line representing the nonlinear regression fit of the data to a model of monomer-dimer equilibrium (Equation 1).

immunofluorescence, mouse monoclonal anti-p65 (sc-8008, Santa Cruz Biotechnology) and rabbit polyclonal anti-FLAG (F7425, Sigma) antibodies were employed.

Reporter Assay—HEK293T cells (5×10^4 /well) were co-transfected with 60 ng of NF- κ B-dependent luciferase reporter plasmid, 10 ng of pRL-TK, and the indicated amount of wild-type or mutant B14 plasmid using FuGENE 6 (Roche Applied Science). The total amount of DNA used per well was kept constant (at either 130 or 320 ng as indicated) by supplementation with the empty vector pCI (Promega). After 24 h, cells were treated with 20 ng/ml IL-1 β or 50 ng/ml TNF α (both PeproTech) or mock-treated for 6 h. Cells were then lysed in Passive Lysis Buffer (Promega), and lysates were analyzed for luciferase activity or by SDS-PAGE and immunoblotting. Firefly luciferase activity was normalized to *Renilla* activity, and values were expressed as the -fold induction compared with untreated cells.

Immunoprecipitation and Immunoblotting—For immunoprecipitation experiments, 293T cells (3×10^6) were transfected with 5 μ g of HA-IKK β and 5 μ g of plasmid expressing wild-type or mutant B14 using the calcium phosphate method. After 24 h, cells were washed once with ice-cold PBS and then lysed in 0.5 ml of lysis buffer (0.5% Nonidet P-40, 50 mM HEPES (pH 7.5), 100 mM NaCl, 1 mM EDTA, 10% (v/v) glycerol, and one protease inhibitor tablet (catalog no. 11 836 170 001, Roche Applied Science)/10 ml of buffer). Lysates were pre-cleared using 10 μ l of protein G-Sepharose beads for 1 h prior to immunoprecipitation. For anti-HA immunoprecipitation, 2.5 μ g of anti-HA mAb was incubated with the lysate overnight at 4 $^{\circ}$ C, and the next day, protein G beads were added and incubated for a further 2 h. For anti-FLAG immunoprecipitation, lysates were incubated with anti-FLAG M2 affinity gel (20 μ l; Sigma) for 2 h at 4 $^{\circ}$ C. The beads were then washed four times with lysis buffer, and the antibody-antigen complexes were eluted from the beads by boiling in 2 \times SDS-PAGE protein loading buffer.

SDS-PAGE and protein transfer onto nitrocellulose membranes were performed according to standard protocols. For

ECL detection, horseradish peroxidase-conjugated secondary antibodies were used, followed by a SuperSignal Western blotting kit (Thermo Scientific). For quantitative Western blotting, IRDye 680-conjugated donkey anti-mouse antibody and IRDye 800-conjugated goat anti-rabbit antibody (LI-COR Biosciences) were used according to the manufacturer's instructions. Membranes were then dried and scanned using the Odyssey infrared imaging system (LI-COR Biosciences). Quantitation was performed using the system software to determine total band intensities on the original scans.

Immunofluorescence—HeLa cells (7×10^4) were seeded onto glass coverslips and transfected (using FuGENE 6) the following day with 50 ng of plasmid expressing wild-type B14 or the Y35E or F130K mutant. After 24 h, cells were either treated with 50 ng/ml TNF α (diluted in warmed minimal essential medium with 2% FBS) or were mock-treated using the same diluent lacking TNF α . After 30 min, the cells were washed three times with ice-cold PBS and then fixed with 4% paraformaldehyde for 5 min on ice, followed by 15 min at room temperature. After washing with PBS, cells were incubated in 150 mM ammonium chloride for 5 min to quench autofluorescence and then permeabilized using 0.1% Triton X-100 (in PBS) for 5 min and blocked using 5% FBS (in PBS) for 30 min. Cells were incubated with primary antibody (anti-p65 diluted 1:50 and anti-FLAG diluted 1:500) for 1 h, washed three times with PBS, and incubated with secondary antibody (Alexa 488-conjugated anti-mouse and Alexa 546-conjugated anti-rabbit) for 45 min in the dark. After further washing, coverslips were mounted in Mowiol/DAPI mounting medium and visualized using a Zeiss Pascal Axioplan LSM confocal microscope.

RESULTS

B14 Exists in Monomer-Dimer Equilibrium in Vitro—B14 crystallizes as a homodimer, the interaction being mediated primarily by interactions between helices 1 and 6 of the two monomers (the 1–6 face) (24). However, the elution profile of B14 during preparative gel filtration suggested that, in solution,

Monomeric VACV B14 Binds IKK β on Its Dimerization Interface

the protein was in monomer-dimer equilibrium (data not shown). This was confirmed by measuring the apparent molar mass of B14 under a range of different concentrations by size-exclusion chromatography with inline MALS (SEC-MALS) (Fig. 1), which showed that the elution volume of the peak fraction decreased and the average molar mass increased with increasing concentrations of B14. This indicated that, in solution, B14 is in monomer-dimer equilibrium, self-associating with modest affinity ($K_D = 20.6 \pm 0.9 \mu\text{M}$).

The observation that B14 dimerization is transient, the protein being monomeric in dilute solution and forming dimers only at relatively high concentration, is consistent with computational analysis performed using PDBePISA (33), which suggested that the dimers of B14 observed in the crystal structure would not constitute a stable complex in solution. However, the hydrophobic nature of the B14 self-association interface (Fig. 2) suggested that this face of the molecule might mediate its interactions with binding partners, such as IKK β , because hydrophobic amino acids are overrepresented at protein-protein interaction interfaces (34). Site-directed mutagenesis was employed to address the possible role of dimerization and/or the contribution of residues at the dimerization interface to IKK β binding. Four mutant forms of B14 were generated in which small or hydrophobic residues at the dimerization interface were replaced with large charged residues: T31K, Y35E, L126E, and F130K (Fig. 2C). The mutant B14 proteins were expressed and purified as described for the wild-type protein (24). Circular dichroism spectropolarimetry confirmed that each adopts an all-helical fold similar to wild-type B14 (data not shown). SEC-MALS analysis confirmed that mutations Y35E, L126E, and F130K all significantly disrupted dimerization: these mutant proteins were monomeric in solution at concentrations at which significant dimerization of the wild-type protein was observed (Fig. 2D). The T31K mutant retained the ability to dimerize, although the affinity of its self-association was significantly reduced (Fig. 2D).

Ability of B14 Mutants to Inhibit NF- κ B Signaling—The ability of mutant B14 to inhibit NF- κ B signaling was determined using reporter assays in which cells were transfected with a plasmid containing a luciferase gene under the control of an NF- κ B-dependent promoter. When cells were co-transfected with the luciferase reporter plasmid together with empty vector, the subsequent addition of either TNF α or IL-1 β stimulated the NF- κ B signaling pathway as indicated by induction of luciferase expression by >50-fold compared with untreated cells (Fig. 3, A and B). Transfection of the wild-type B14 plasmid in place of the empty vector inhibited reporter activity substantially ($p < 0.01$) irrespective of the stimulatory ligand (TNF α or IL-1 β), consistent with a previous reports (21). Notably, the Y35E mutant blocked NF- κ B signaling as strongly as wild-type B14. In contrast, the F130K mutant did not significantly inhibit luciferase reporter levels (Fig. 3A) or was associated with quantitatively minor yet statistically significant reductions in reporter activity (Fig. 3B). Immunoblotting was performed in parallel and showed that all proteins were well expressed (Fig. 3, A and B). To compare more accurately the activity of the mutant and

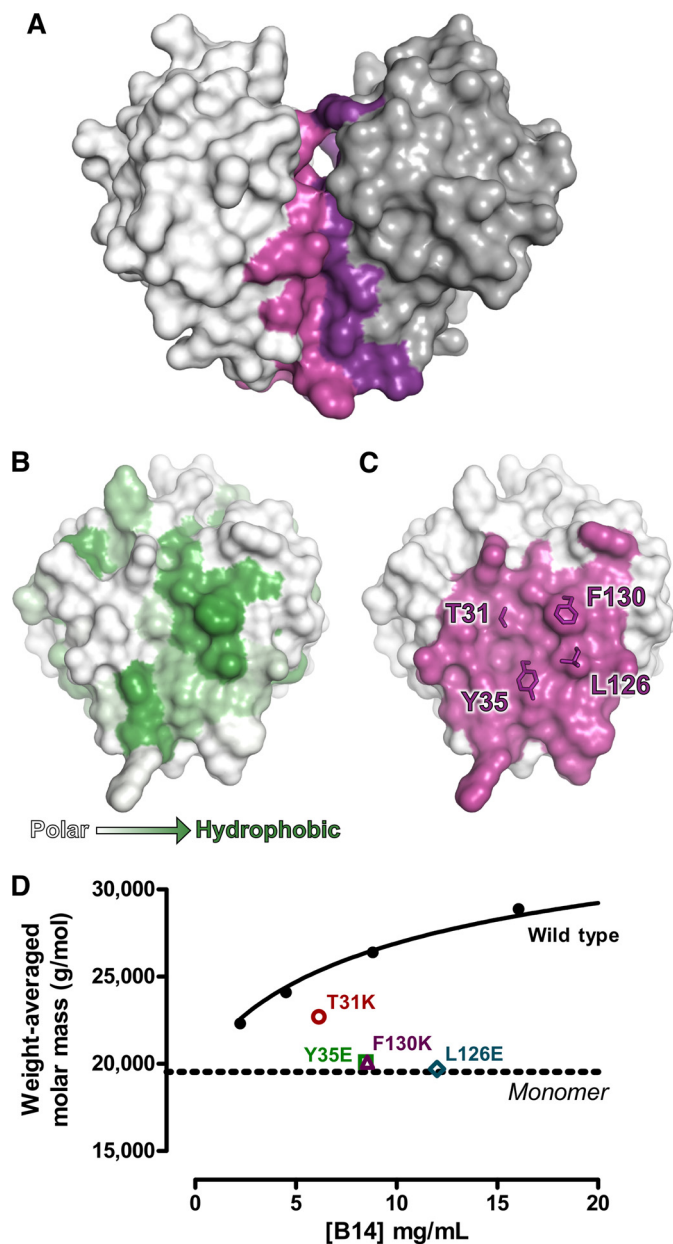


FIGURE 2. Mutation of residues at the B14 dimer interface disrupts self-association. A, the molecular surface of B14 is shown (Protein Data Bank code 2VVY), with the individual monomers colored light and dark gray and residues at the dimerization interface colored light and dark magenta. B, the dimerization interface of B14 is shown colored by surface amino acid hydrophobicity from white (polar) to green (hydrophobic). C, the B14 dimerization interface is shown, with residues that participate in the self-association colored magenta. The side chains of residues mutated in this study are shown as sticks. D, the weight average molar masses of wild-type B14 and mutants are plotted versus concentration. The solid line represents the nonlinear regression fit of the wild-type data as described in the legend to Fig. 1.

wild-type B14 proteins, a dose-response experiment was conducted (Fig. 3C). As a control, the VACV C6 protein, another predicted member of the VACV Bcl-2 family (24), was analyzed in parallel and was found not to antagonize the NF- κ B pathway.⁸ All of the B14 proteins were significantly inhibitory relative to the empty vector, except F130K at 30 ng and the negative control C6 at 30 and 60 ng ($p < 0.01$) (Fig.

⁸ R. P. Sumner, personal communication.

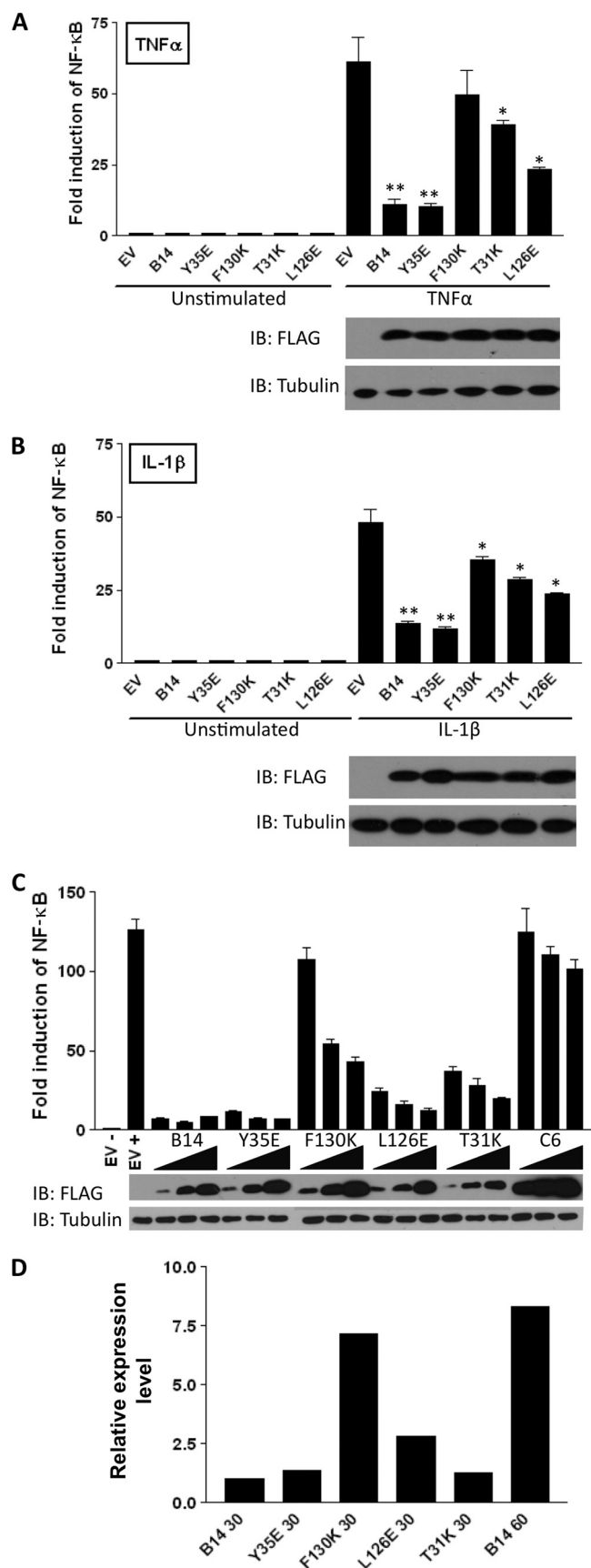


FIGURE 3. Reporter assays for inhibition of NF- κ B activation by B14 mutants. 293T cells were transfected with 60 ng of NF- κ B-luciferase reporter plasmid, 10 ng of pRL-TK internal control, and either 60 ng (A and B) or 30, 60,

30 ng (C) of empty vector (EV) or FLAG-tagged wild-type B14 or mutant Y35E, F130K, L126E, or T31K. After 24 h, cells were stimulated with either 50 ng/ml TNF α (A and C) or 20 ng/ml IL-1 β (B) for 6 h or were left unstimulated. In C, - and + denote unstimulated and TNF α -stimulated conditions, respectively, for the empty vector, and C6 is a FLAG-tagged VACV protein negative control. Luciferase activity was measured and normalized to the *Renilla* activity for each well. The mean \pm S.D. ($n = 3$) is shown for the -fold induction of NF- κ B-dependent luciferase activity relative to uninduced cells transfected with the same plasmid mixture. *, $p < 0.05$; **, $p < 0.01$, significant difference (Student's *t* test) relative to the empty vector for A and B. Immunoblotting (IB) was done in parallel with reporter assays using pooled lysates from triplicate transfections and antibodies as indicated. The immunoblot panels in A–C used conventional ECL detection. D, quantitation of wild-type and mutant B14 expression in the assay shown in C. Expression levels are shown for all mutants transfected at 30 ng and for wild-type B14 transfected at 30 and 60 ng (as indicated) under TNF α -stimulated conditions. Values were derived from the quantitative immunoblot (Odyssey system) shown in supplemental Fig. S1. FLAG expression levels were normalized to the tubulin expression in each lysate and are given relative to wild-type B14 protein transfected at 30 ng.

Next, the Y35E and F130K mutants were tested using an alternative functional assay in which their effect upon the subcellular localization of p65 was assessed using immunofluorescence. In unstimulated HeLa cells, p65 was detected within the cytoplasm irrespective of whether the cells were untransfected or expressed wild-type B14 or mutant F130K or Y35E (Fig. 4A, – panels). Upon stimulation with TNF α , p65 translocated to the nucleus in untransfected (*i.e.* FLAG-negative) cells. However, in cells expressing wild-type B14, the TNF α -stimulated nuclear translocation of p65 was blocked, and p65 was retained in the cytoplasm. This is consistent with B14 inhibiting the phosphorylation and subsequent degradation of I κ B α (21), which leads to continued association of the p65 transcription factor and its inhibitor I κ B α in the cytoplasm. Quantification revealed that nuclear p65 staining was seen in only 3% of B14-expressing cells and

or 120 ng (C) of empty vector (EV) or FLAG-tagged wild-type B14 or mutant Y35E, F130K, L126E, or T31K. After 24 h, cells were stimulated with either 50 ng/ml TNF α (A and C) or 20 ng/ml IL-1 β (B) for 6 h or were left unstimulated. In C, - and + denote unstimulated and TNF α -stimulated conditions, respectively, for the empty vector, and C6 is a FLAG-tagged VACV protein negative control. Luciferase activity was measured and normalized to the *Renilla* activity for each well. The mean \pm S.D. ($n = 3$) is shown for the -fold induction of NF- κ B-dependent luciferase activity relative to uninduced cells transfected with the same plasmid mixture. *, $p < 0.05$; **, $p < 0.01$, significant difference (Student's *t* test) relative to the empty vector for A and B. Immunoblotting (IB) was done in parallel with reporter assays using pooled lysates from triplicate transfections and antibodies as indicated. The immunoblot panels in A–C used conventional ECL detection. D, quantitation of wild-type and mutant B14 expression in the assay shown in C. Expression levels are shown for all mutants transfected at 30 ng and for wild-type B14 transfected at 30 and 60 ng (as indicated) under TNF α -stimulated conditions. Values were derived from the quantitative immunoblot (Odyssey system) shown in supplemental Fig. S1. FLAG expression levels were normalized to the tubulin expression in each lysate and are given relative to wild-type B14 protein transfected at 30 ng.

Monomeric VACV B14 Binds IKK β on Its Dimerization Interface

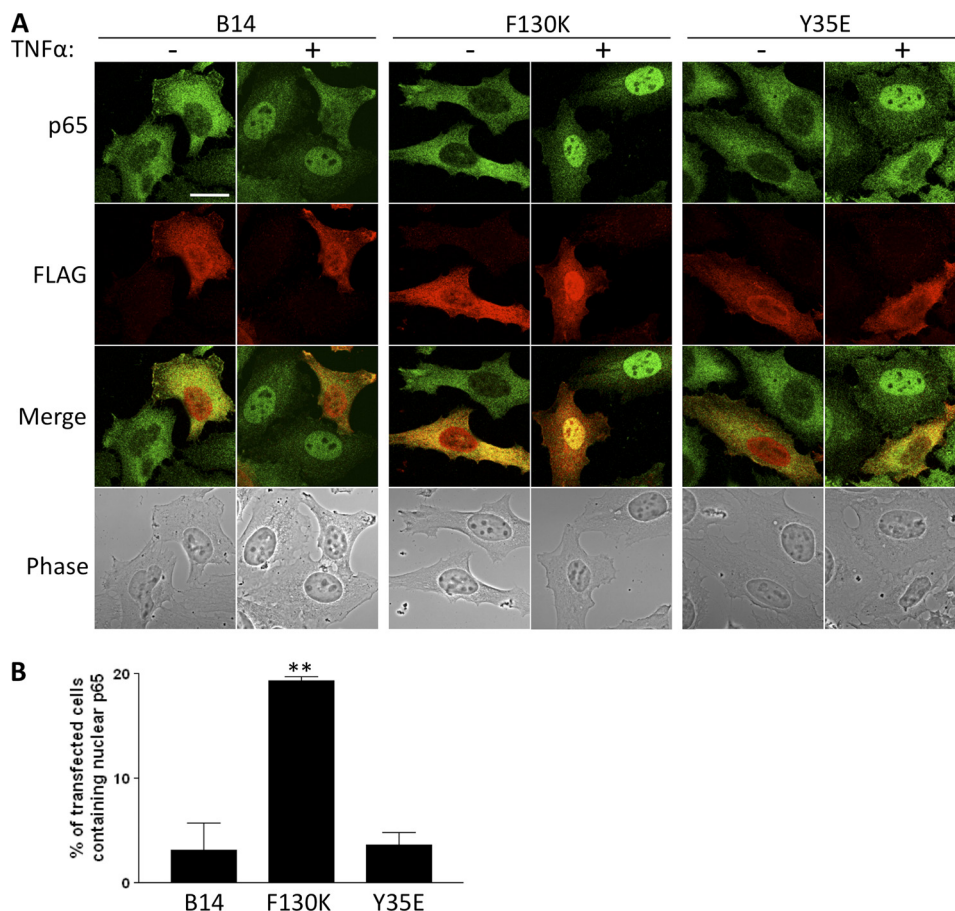


FIGURE 4. Nuclear translocation of p65. HeLa cells were transfected with FLAG-tagged wild-type B14 or mutant F130K or Y35E (50 ng). After 24 h, cells either were stimulated with 50 ng/ml TNF α (+) or were mock-treated (-), and 30 min later, the cells were fixed and processed for immunofluorescence to detect p65 and the FLAG epitope. p65 and FLAG were detected using Alexa 488- and Alexa 568-conjugated antibodies, respectively. *A*, immunofluorescence images of representative fields. Scale bar = 20 μ m. *B*, quantification of p65 translocation showing the proportion of FLAG-positive cells that contained strong nuclear p65 staining for cells transfected with wild-type B14 or mutant F130K or Y35E. For each plasmid, three independently transfected slides were counted in a blinded manner to give the mean \pm S.D. ($n = 100$ cells/slide). **, $p < 0.01$, significant difference (Student's *t* test) relative to wild-type B14.

that p65 was restricted to the cytoplasm in the remaining 97% (Fig. 4*B*). Likewise, in cells expressing the Y35E mutant, p65 was retained in the cytoplasm, and only very few cells (4%) had p65 staining within the nucleus (Fig. 4, *A* and *B*). However, for F130K, the proportion of transfected (*i.e.* FLAG-positive) cells containing nuclear p65 after TNF α stimulation was 19%, significantly higher than for wild-type B14 ($p < 0.001$) (Fig. 4, *A* and *B*). Thus, F130K was unable to block TNF α -stimulated nuclear translocation of p65 as efficiently as wild-type B14. In sum, the analysis of nuclear translocation of p65 supported the reporter assay data in showing that the F130K mutation caused functional impairment, whereas the Y35E mutation did not impair the ability of the VACV B14 protein to block NF- κ B-dependent signaling.

Ability of Mutants to Bind IKK β —B14 binds to IKK β and thereby prevents IKK β phosphorylation and activation of kinase activity. Having characterized the ability of the B14 dimer interface mutants to inhibit NF- κ B nuclear translocation and NF- κ B-dependent transcriptional responses, the interactions of the mutants with IKK β were investigated by immunoprecipitation. 293T cells were transfected with HA-tagged IKK β and FLAG-tagged B14 (wild-type or mutant), and cyto-

plasmic lysates were prepared. As a control, cells transfected with the FLAG-tagged VACV E3 protein were analyzed in parallel. Monoclonal anti-HA antibody precipitated HA-IKK β in each case, but only FLAG-tagged wild-type B14 and mutant Y35E were co-immunoprecipitated with HA-IKK β , whereas mutant F130K and the VACV E3 protein were not (Fig. 5*A*). The interaction between B14 and IKK β demonstrated in these experiments was specific because no B14 was co-immunoprecipitated with the same concentration of an isotype-matched control antibody (Fig. 5*A*). The reciprocal immunoprecipitation was performed using monoclonal anti-FLAG antibody and again showed that IKK β bound wild-type B14 and Y35E but not F130K or E3 (Fig. 5*B*). The L126E and T31K mutants, which were shown to be intermediate in their ability to inhibit NF- κ B signaling (Fig. 3), were able to bind IKK β (Fig. 5*B*). However, less IKK β protein was co-immunoprecipitated with these mutants compared with B14 or Y35E, despite equivalent levels of IKK β within the input lysates. These differences were quantified using the Odyssey Western blotting system (Fig. 5*C* and Fig. S2). Data are expressed as the amount of precipitated IKK β relative to the amount of input IKK β , but similar data were obtained when normalization was performed relative to the amount of

Monomeric VACV B14 Binds IKK β on Its Dimerization Interface

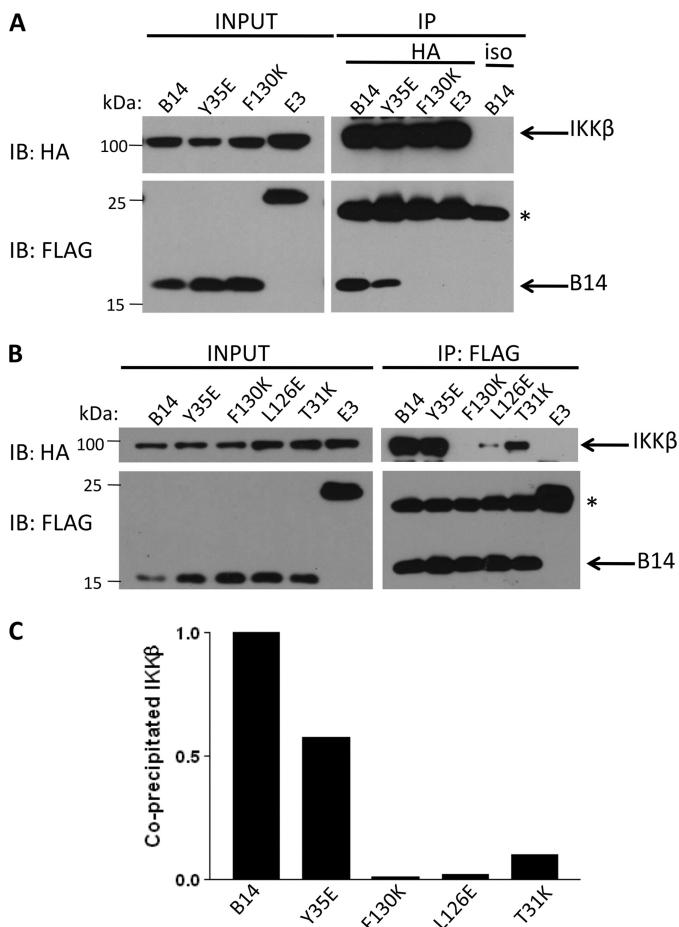


FIGURE 5. Binding of IKK β by wild-type and mutant B14 proteins. 293T cells were co-transfected with HA-tagged IKK β and FLAG-tagged wild-type B14 or mutant Y35E, F130K, L126E, or T31K or the negative control VACV E3 protein. After 24 h, lysates from these cells were immunoprecipitated using either monoclonal anti-HA antibody or an isotype-matched control antibody against CD45 (*iso*) (A) or monoclonal anti-FLAG antibody (B and C). The immunoprecipitated (IP) and input proteins were resolved by SDS-PAGE on a 12% gel and then analyzed by immunoblotting (IB) with the indicated antibodies. Size markers are indicated on the left (in kilodaltons), and the identity of the protein bands is indicated on the right. The asterisk marks the position of the IgG light chain. C, after immunoprecipitation using anti-FLAG antibody, the amount of HA-IKK β that co-precipitated with the wild-type or mutant B14 proteins was measured by quantitative immunoblotting (LI-COR; blot shown in supplemental Fig. S2). For each protein, the amount of co-precipitated IKK β was normalized to the amount of IKK β protein in the input lysates and then expressed relative to wild-type B14.

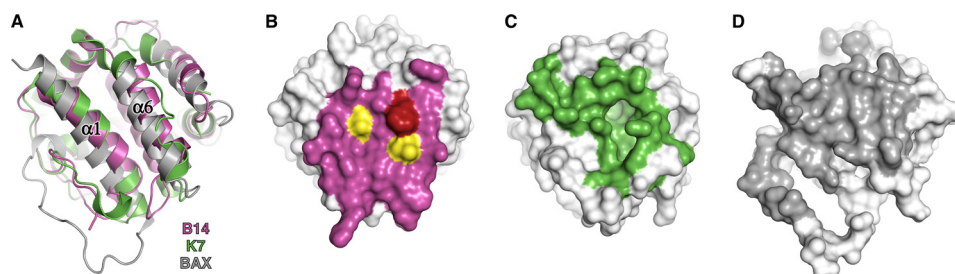


FIGURE 6. The B14 dimerization-IKK β interaction interface is topologically similar to protein-protein interaction interfaces of VACV K7 and human BAX. A, the overlaid structures of Bcl-2-like proteins B14 (purple; Protein Data Bank code 2VVY), K7 (green; code 3JRV), and BAX (gray; code 2K7W) are shown as ribbons. B, the molecular surface of B14 is shown (white) in the same orientation as A, with residues involved in dimerization (purple) and residues that reduce (T31K and L126E; yellow) or abolish (F130K; red) interaction with IKK β highlighted. C, the molecular surface of K7 is shown (white), with residues that interact with DDX3 (green) highlighted. D, the molecular surface of BAX is shown (white), with residues that interact with the BIM SAHB peptide (gray) highlighted.

input FLAG-tagged B14 instead. Y35E co-precipitated approximately half as much IKK β as wild-type B14, whereas the binding of IKK β to F130K, undetectable using conventional ECL, was found to be only 1% of that of wild-type B14. The considerably reduced binding of the L126E mutant to IKK β compared with wild-type B14 was nevertheless sufficient to mediate significant inhibition of NF- κ B reporter assays.

DISCUSSION

The IKK complex lies at the nexus of NF- κ B signaling: distinct upstream signaling pathways initiated by various different pro-inflammatory stimuli converge upon the IKK complex to lead to NF- κ B activation. Thus, inhibiting the IKK complex is a particularly effective strategy to diminish NF- κ B-mediated pro-inflammatory and immunostimulatory responses. This strategy is adopted by the VACV protein B14, which binds and inhibits IKK β (21), the subunit of the IKK complex critical for phosphorylation of the inhibitor of NF- κ B (I κ B α) in response to pro-inflammatory stimuli (1, 10). The structure of B14 revealed it to be a Bcl-2-like protein that crystallizes as a dimer (24). In the present study, targeted mutagenesis was used to determine the functional relevance of B14 dimerization and to map the region of B14 that interacts with IKK β .

The elution profile of B14 during preparative gel filtration experiments suggested that, in solution, not all B14 forms dimers. This observation was confirmed by SEC-MALS analysis, which demonstrated that, in solution, B14 exists in a concentration-dependent equilibrium between monomeric and dimeric states and that the strength of self-association is relatively modest ($K_D = 20.6 \pm 0.9 \mu\text{M}$) (Fig. 1). The transient nature of the self-association suggested that dimerization of B14 might involve the same surface (the 1–6 face) that mediates interactions between B14 and other proteins; in the absence of its correct binding partner, dimerization of B14 could shield the hydrophobic protein-protein interaction interface of B14 from the (polar) solvent. To address the physiological relevance of dimerization and the residues by which it is mediated, point mutations were designed to disrupt B14 self-association by increasing the charge at the dimerization interface (Y35E, L126E, T31K, and F130K). Recombinant protein was synthesized and purified for all the mutants, and circular dichroism analysis confirmed that each was correctly folded. SEC-MALS experiments showed that B14 mutants Y35E, F130K, and L126E

Monomeric VACV B14 Binds IKK β on Its Dimerization Interface

no longer dimerized in solution, whereas the propensity of mutant T31K to form dimers was significantly reduced compared with the wild-type protein (Fig. 2D). However, disruption of dimerization did not necessarily abolish the ability of the B14 mutants to bind IKK β because the interaction of the Y35E mutant with IKK β was comparable with that of the wild-type protein (Fig. 5B). This demonstrates that the IKK β -binding site does not span two monomer subunits of B14. Given that the monomeric Y35E mutant inhibited NF- κ B signaling to the same extent as wild-type B14 (Figs. 3 and 4), B14 monomers are fully functional and are likely to represent the physiologically relevant state of the protein.

In contrast to the Y35E mutant, the F130K mutant did not significantly block NF- κ B signaling (Fig. 3). This functional impairment occurred concomitantly with loss of IKK β binding (Fig. 5). This clear correlation between the extent of IKK β binding and NF- κ B inhibition for the mutant protein provides further evidence that B14 antagonizes the NF- κ B pathway via its direct interaction with the IKK β component of the IKK complex. Because F130K was nonfunctional despite being well folded, we propose that Phe-130 forms part of the IKK β -binding interface of B14. The T31K and L126E mutants were intermediate in their activity, both capable of binding IKK β and inhibiting NF- κ B signaling, but to a lesser extent compared with wild-type B14. It is therefore possible that these residues are in the vicinity of, but peripheral to, the IKK β -binding interface of B14. Taken together, these data indicate that the interaction face for IKK β on B14 overlaps the dimerization interface (shown in Fig. 2C) and that hydrophobic residues (*i.e.* Phe-130), which mediate B14-IKK β interaction under physiological conditions, contribute instead to homodimerization when B14 is in concentrated solution in the absence of its binding partner IKK β .

In addition to B14, the structures of four other VACV Bcl-2-like proteins have been determined recently: N1 (25, 26), A52 (24), F1 (27), and K7 (28). Of these, three (A52, N1, and F1) form dimers both *in crystallo* and *in vitro* (24, 27).⁹ However, the Bcl-2-like VACV K7 protein exists as a monomer in solution (28) and binds its partner (DDX3) at the 1–6 face, which is equivalent to the surface that forms the dimerization interfaces of A52 (35) and B14 (Fig. 6). In the case of K7, electrostatic repulsion by the high density of negatively charged residues on the DDX3 interaction face presumably prohibits dimerization (35). Furthermore, it was shown recently that the human Bcl-2 family protein BAX is activated by binding of the helical BIM SAHB peptide on the 1–6 face of the protein (36). This face is distinct from the canonical BH3 peptide-binding groove formed by helices 2–5, instead corresponding to the B14 dimerization interface (Fig. 6). The 1–6 face of Bcl-2-like proteins seems to favor participation in either homo- or heterotypic protein-protein interactions, underscoring the utility of the Bcl-2-like fold as a scaffold that can carry a variety of different

immunomodulatory functions by mediating interactions with distinct cellular binding partners (24).

Acknowledgments—We thank Janet Deane for assistance with CD experiments, Geoff Sutton for assistance with SEC-MALS, and Bernard Kelly for helpful discussions.

REFERENCES

- Hayden, M. S., and Ghosh, S. (2004) *Genes Dev.* **18**, 2195–2224
- Chen, Z., Hagler, J., Palombella, V. J., Melandri, F., Scherer, D., Ballard, D., and Maniatis, T. (1995) *Genes Dev.* **9**, 1586–1597
- Chen, Z. J., Parent, L., and Maniatis, T. (1996) *Cell* **84**, 853–862
- Yaron, A., Gonen, H., Alkalay, I., Hatzubai, A., Jung, S., Beyth, S., Mercurio, F., Manning, A. M., Ciechanover, A., and Ben-Neriah, Y. (1997) *EMBO J.* **16**, 6486–6494
- Mercurio, F., Zhu, H., Murray, B. W., Shevchenko, A., Bennett, B. L., Li, J., Young, D. B., Barbosa, M., Mann, M., Manning, A., and Rao, A. (1997) *Science* **278**, 860–866
- Rothwarf, D. M., Zandi, E., Natoli, G., and Karin, M. (1998) *Nature* **395**, 297–300
- Yamaoka, S., Courtois, G., Bessia, C., Whiteside, S. T., Weil, R., Agou, F., Kirk, H. E., Kay, R. J., and Israël, A. (1998) *Cell* **93**, 1231–1240
- Häcker, H., and Karin, M. (2006) *Sci. STKE* 2006, re13
- Wang, C., Deng, L., Hong, M., Akkaraju, G. R., Inoue, J., and Chen, Z. J. (2001) *Nature* **412**, 346–351
- Israël, A. (2010) *Cold Spring Harbor Perspect. Biol.* **2**, a000158
- Randall, R. E., and Goodbourn, S. (2008) *J. Gen. Virol.* **89**, 1–47
- Alcamí, A., Khanna, A., Paul, N. L., and Smith, G. L. (1999) *J. Gen. Virol.* **80**, 949–959
- Alcamí, A., and Smith, G. L. (1992) *Cell* **71**, 153–167
- Bowie, A., Kiss-Toth, E., Symons, J. A., Smith, G. L., Dower, S. K., and O'Neill, L. A. (2000) *Proc. Natl. Acad. Sci. U.S.A.* **97**, 10162–10167
- Harte, M. T., Haga, I. R., Maloney, G., Gray, P., Reading, P. C., Bartlett, N. W., Smith, G. L., Bowie, A., and O'Neill, L. A. (2003) *J. Exp. Med.* **197**, 343–351
- Stack, J., Haga, I. R., Schröder, M., Bartlett, N. W., Maloney, G., Reading, P. C., Fitzgerald, K. A., Smith, G. L., and Bowie, A. G. (2005) *J. Exp. Med.* **201**, 1007–1018
- Shisler, J. L., and Jin, X. L. (2004) *J. Virol.* **78**, 3553–3560
- Schröder, M., Baran, M., and Bowie, A. G. (2008) *EMBO J.* **27**, 2147–2157
- DiPerna, G., Stack, J., Bowie, A. G., Boyd, A., Kotwal, G., Zhang, Z., Arvikar, S., Latz, E., Fitzgerald, K. A., and Marshall, W. L. (2004) *J. Biol. Chem.* **279**, 36570–36578
- Gedey, R., Jin, X. L., Hinthong, O., and Shisler, J. L. (2006) *J. Virol.* **80**, 8676–8685
- Chen, R. A., Ryzhakov, G., Cooray, S., Randow, F., and Smith, G. L. (2008) *PLoS Pathog.* **4**, e22
- Chen, R. A., Jacobs, N., and Smith, G. L. (2006) *J. Gen. Virol.* **87**, 1451–1458
- Assarsson, E., Greenbaum, J. A., Sundström, M., Schaffer, L., Hammond, J. A., Pasquetto, V., Oseroff, C., Hendrickson, R. C., Lefkowitz, E. J., Tschärke, D. C., Sidney, J., Grey, H. M., Head, S. R., Peters, B., and Sette, A. (2008) *Proc. Natl. Acad. Sci. U.S.A.* **105**, 2140–2145
- Graham, S. C., Bahar, M. W., Cooray, S., Chen, R. A., Whalen, D. M., Abrescia, N. G., Alderton, D., Owens, R. J., Stuart, D. I., Smith, G. L., and Grimes, J. M. (2008) *PLoS Pathog.* **4**, e1000128
- Aoyagi, M., Zhai, D., Jin, C., Aleshin, A. E., Stec, B., Reed, J. C., and Lidington, R. C. (2007) *Protein Sci.* **16**, 118–124
- Cooray, S., Bahar, M. W., Abrescia, N. G., McVey, C. E., Bartlett, N. W., Chen, R. A., Stuart, D. I., Grimes, J. M., and Smith, G. L. (2007) *J. Gen. Virol.* **88**, 1656–1666
- Kvansakul, M., Yang, H., Fairlie, W. D., Czabotar, P. E., Fischer, S. F., Perugini, M. A., Huang, D. C., and Colman, P. M. (2008) *Cell Death Differ.* **15**, 1564–1571
- Kalverda, A. P., Thompson, G. S., Vogel, A., Schröder, M., Bowie, A. G., Khan, A. R., and Homans, S. W. (2009) *J. Mol. Biol.* **385**, 843–853

⁹C. T. O. Benfield, D. S. Mansur, L. E. McCoy, B. J. Ferguson, M. W. Bahar, A. P. Oldring, J. M. Grimes, D. I. Stuart, S. C. Graham, and G. L. Smith, unpublished data.

Monomeric VACV B14 Binds IKK β on Its Dimerization Interface

29. Bahar, M. W., Graham, S. C., Chen, R., Cooray, S., Smith, G. L., Stuart, D. I., and Grimes, J. M. (March 17, 2011) *J. Struct. Biol.* 10.1016/j.jsb.2011.03.010
30. Bartlett, N., Symons, J. A., Tschärke, D. C., and Smith, G. L. (2002) *J. Gen. Virol.* **83**, 1965–1976
31. Wyatt, P. J. (1993) *Anal. Chim. Acta* **272**, 1–40
32. Krissinel, E., and Henrick, K. (2004) *Acta Crystallogr. D Biol. Crystallogr.* **60**, 2256–2268
33. Krissinel, E., and Henrick, K. (2007) *J. Mol. Biol.* **372**, 774–797
34. Jones, S., and Thornton, J. M. (1996) *Proc. Natl. Acad. Sci. U.S.A.* **93**, 13–20
35. Oda, S., Schröder, M., and Khan, A. R. (2009) *Structure* **17**, 1528–1537
36. Gavathiotis, E., Suzuki, M., Davis, M. L., Pitter, K., Bird, G. H., Katz, S. G., Tu, H. C., Kim, H., Cheng, E. H., Tjandra, N., and Walensky, L. D. (2008) *Nature* **455**, 1076–1081